Who gets the Maximal Extractable Value? A Dynamic Sharing Blockchain Mechanism

Anonymous Author(s)
Submission Id: 1083

ABSTRACT

Maximal Extractable Value (MEV) has emerged as a new frontier in the design of blockchain systems. The marriage between decentralization and finance gives the power to block producers (a.k.a., miners) not only to select and add transactions to the blockchain but, crucially, also to order them so as to extract as much financial gain as possible for themselves. Whilst this price may be unavoidable for the service provided by block producers, users of the chain may in the long run prefer to use less predatory systems.

In this paper, we propose to make the *MEV extraction rate* part of the protocol design space. Our aim is to leverage this parameter to maintain a healthy balance between miners (who need to be compensated) and users (who need to feel encouraged to transact). Inspired by the principles introduced by EIP-1559 for transaction fees, we design a dynamic mechanism which updates the MEV extraction rate with the goal of stabilizing it at a target value. We analyse the evolution of this dynamic mechanism under various market conditions and provide formal guarantees about its long-term performance. Our results show that even when the system behavior is provably chaotic, the dynamics guarantee long-term liveness (survival) and robustness of the system. The main takeaway from our work is that the proposed system exhibits desirable behavior (near-optimal performance) even when it operates in out of equilibrium conditions that are often met in practice. Our work establishes, the first to our knowledge, dynamic framework for the integral problem of MEV sharing between extractors and users.

KEYWORDS

blockchain, maximal extractable value, out-of-equilibrium analysis, chaotic dynamical systems, markets, mechanism design

ACM Reference Format:
Anonymous Author(s). 2024. Who gets the Maximal Extractable Value? A Dynamic Sharing Blockchain Mechanism. In *Proc. of the 23rd International Conference on Autonomous Agents and Multiagent Systems (AAMAS 2024), Auckland, New Zealand, May 6 – 10, 2024*, IFAAMAS, 11 pages.

1 INTRODUCTION

Smart contract blockchains, such as Ethereum [40], Cardano [22] and Tezos [16], unveiled the ability to construct flexible financial products on top of blockchains and led to emergence of *Decentralized Finance* (DeFi). DeFi supports most applications available in traditional finance such as asset exchanges, trading of tokens through Decentralized Exchanges (DEXes), loans, decentralized governance, and stablecoins (currency boards) [41].

Proc. of the 23rd International Conference on Autonomous Agents and Multiagent Systems (AAMAS 2024), N. Alechina, V. Dignum, M. Dastani, J.S. Sichman (eds.), May 6 – 10, 2024, Auckland, New Zealand.

However, block-creators, e.g., miners in Proof of Work (PoW), or validators in Proof of Stake (PoS) networks, have unilateral power to decide which transactions to execute and in which order. This unfolds a rich strategy space to extract additional profit, usually at the expense of users. *Maximal Extractable Value* (MEV) is any type of excess profit a block creator can obtain by adding, ordering, or censoring transactions [8]. The multiple forms of MEV include frontrunning, arbitrage and sandwich attacks in DEXes [14], liquidations [18, 34], cross-chain MEV [31] and NFT-mint front running [14]. While many of these practices have been prevented or regulated in traditional finance (e.g., frontrunning is known to breach certain MiFID II standards, such as, best execution — fca.org), the lack of centralized authorities renders such mechanisms of little or no practical relevance to the DeFi setting.

In current smart-contract blockchains, MEV constitutes an integral source of concern. The reason is that even though MEV is produced by the economic activity of users (MEV generators), in most cases, the extracted amount goes to other agents of the system (MEV extractors). Resolving this tension is far from straightforward. Extreme solutions, in which all MEV goes either back to users or to block-creators, are shown to adversely affect the behaviour of the opposite group and end up compromising participation and system security [7, 8, 35].

Hence, the question of how to share the welfare between these two groups, i.e., users and block creators, constitutes a central problem in current blockchain research and practice [11, 13]. The current debate around MEV *sharing* or mitigation involves two main schools of thought. The first is the *anti-MEV* approach, which states that MEV is harmful and its exploitation must be prevented or mitigated [19–21]. The second is the *pro-MEV* approach which argues that, despite its negative externalities, MEV is inevitable in permissionless blockchains, and sometimes it even improves the quality of executing transactions [7, 11, 23, 30]. However, despite the intense interest of the blockchain community to resolve this problem, to the best of our knowledge, a rigorous proposal with provable guarantees remains elusive.

Our Approach and Results. In this work, we take a neutral approach towards MEV and propose a mechanism to balance the two extreme positions by enshrining MEV sharing in the protocol design. The key element to achieve this is a variable MEV *extraction rate* that determines the fraction of MEV that is retained by miners,[1] with the rest going back to users. For example, an MEV extraction rate of 1 (0, resp.) means that all MEV goes to miners (users, resp.).

The aim of the MEV extraction rate is to balance the participation of users and miners, expressed in monetary terms, to a predetermined target ratio and is updated after every block following a

[1] Due to its common usage, we will also use the term *miners* for simplicity as a shorthand of all parties that are involved in the process of *block creation* and MEV extraction, such as validators, block proposers, builders, searchers, etc. [29].

dynamic update rule. The intensity of the updates is regulated by an *adjustment parameter* that is part of the design space of the mechanism. In simple terms, the rule increases (decreases, respectively) the MEV extraction rate if the ratio of miner/user participation is lower (higher, respectively) than desired. To measure deviations from the target, we consider the winning bid of the auction held for the creation of the last block as a proxy of the extracted MEV.[2] This dynamic update rule is inspired by the design principles of EIP-1559 that have proven successful in regulating transaction fee markets under similar conditions [24, 25, 37, 38], and the trade-off between the goals of users (bidders) and miners (auctioneers) as studied in the context of conventional auctions [9, 28].[3]

Our objective in this paper is to study the evolution and performance of the above mechanism. In particular, to contribute to the ongoing debate about MEV, our motivating questions are the following: (1) can a protocol-determined, dynamically-updated MEV extraction rate balance the conflicting participation incentives of users and miners, and (2) can the design principles of EIP-1559 be useful in accomplishing this task?

Our findings provide significant evidence that we can answer both questions affirmatively. Specifically, our formal analysis of the long-term evolution of the dynamic mechanism shows that the system exhibits one of the following behaviors depending on the intensity of the updates, as these are determined by the value of the adjustment parameter: (i) *low* intensities: convergence to an optimal MEV extraction rate that achieves the target participation ratio and which is strictly between 0 and 1, (ii) *intermediate* intensities: periodic behavior or provable chaos (Theorem 3.9) or (iii) *large* intensities: collapse to extraction rates of either 0 or 1 in which case one of the two groups of this two-sided economy abandons the system. In Theorem 3.3 and Theorem 3.4, we establish formal threshold bounds on the intensity of the updates for which the system either avoids the degenerate states of 0 and 1 and remains *live*, i.e., avoids regime (iii), or equilibrates (stabilizes) at the target MEV extraction rate, i.e., reaches regime (i), respectively.

Turning to system performance, we mathematically quantify deviations from target participation levels and show that they remain bounded for a broad range of realistic market conditions and parameterizations (Theorem 4.2). This means that the system maintains a healthy proportion between miners and users. The main takeaway is that this desirable behavior is formally exhibited not only when the system equilibrates, i.e., when it stabilizes at the target extraction rate, a condition that may rarely be met in practice, but, also, when it operates under *out-of-equilibrium (chaotic) conditions*.

Technically, our paper is most closely related to the literature on complex dynamics that have been previously studied in various theoretical settings [15, 32, 33] and, recently, also in market [6] and blockchain settings [24, 25]. Our current work extends these frameworks to include rigorous guarantees on market-liveness and long-term system performance. In stark contrast to conventional equilibrium analysis, which offers little or no insight on non-equilibrium regimes, such guarantees are critical to ensure the long-term survival and robustness of systems with strong practical orientation [26].

2 MODEL

We consider a two-sided market consisting of users (or MEV generators) who submit transactions on the one side and miners (or MEV extractors) who process these transactions on the other side. Here, the term *miners* is used as a general term to describe all MEV extractors including proposers, builders, searchers.[4] The two sides are described in terms of their total participating stake, denoted by U for users and by M for miners. In other words, U and M denote the maximum potential participation of users and miners, respectively, measured in monetary terms (transaction volume for users and locked stake for miners) during the time-period under consideration.[5]

The participation of users and miners in the market depends on the current MEV extraction rate, denoted by $\lambda \in [0, 1]$. Higher (lower) values of λ indicate more (less) aggressive extraction by miners and, hence, a more (less) hostile environment for users. Equivalently, one may think of $1 - \lambda$ as the fraction of MEV that is returned to users through rebates, direct payments or other on or off-chain vehicles. Each user and miner has a certain tolerance on λ. Thus, if a user (miner) sees an MEV extraction rate higher (lower) than what they can tolerate, they do not participate in the market. The *tolerance distributions* of users and miners are denoted by $F(\lambda)$ and $G(\lambda)$, respectively. Based on the above, the users that participate in the market for a given λ are $U \cdot \bar{F}(\lambda)$, where $\bar{F}(\lambda) := 1 - F(\lambda)$ and the miners are $M \cdot G(\lambda)$. We assume that the support of F, G is included in $[0, 1]$ and that both F, G are strictly increasing and differentiable with probability density functions $f = F', g = G'$, respectively.[6]

To incorporate the MEV extraction rate as part of the protocol design space, we make the following design choices:

- The MEV extraction rate is dynamically updated after every block. This generates a sequence of MEV extraction rates, $(\lambda_t)_{t \geq 0}$, where t indicates the block height (time).
- The intensity of the updates between consecutive blocks is regulated by a parameter d that can be chosen by the designer.
- The designer can set a desired (optimal) balance between users and miners in the market denoted by T (target). This means that the designer is seeking to find a λ^* such that $U \cdot \bar{F}(\lambda^*) = T \cdot M \cdot G(\lambda^*)$.
- The boundary MEV extraction rates of $\lambda = 0$ and $\lambda = 1$ correspond to steady states in which the two-sided market collapses to having either only miners ($\lambda = 1$) or only users ($\lambda = 0$).

Based on the above desiderata, and inspired by EIP-1559 transaction fee design, we consider the following dynamic update rule to govern

[2] The estimation of MEV is not *the* focus of our model. In any case, current research suggests that winning bids in MEV-boost auctions [10, 12] or experimental methods [2, 3, 17, 35] provide accurate estimates or tight lower bounds to the actual MEV.

[3] It is worth highlighting that to measure deviations from its target and to adjust its updates accordingly, EIP-1559 uses as (on-chain) proxy of current demand the size of the last block [5].

[4] To extract MEV, miners can also submit transactions, but the precise mechanics in which the extraction occurs do not affect our analysis.

[5] It is safe to assume that the amounts U and M remain relatively stable in the short/medium-term, but can undergo more significant changes in the long-term. The impact of such changes in the dynamics of the current paper is explained in the appendix.

[6] The strict monotonicity and differentiability assumptions are common in the economics literature and only serve to avoid edge cases that complicate the analysis without adding much intuition. Our results readily extend to more complex distributions.

the evolution of the MEV extraction rates, λ_t:

$$\lambda_{t+1} := \lambda_t + d\lambda_t(1-\lambda_t)\cdot(U\cdot\bar{F}(\lambda_t) - T\cdot M\cdot G(\lambda_t)).$$

In the update function of the right hand side, the terms $\lambda_t, (1-\lambda_t)$ ensure that $\lambda = 0$ and $\lambda = 1$ are fixed points of the system and the term $U\cdot\bar{F}(\lambda_t) - T\cdot M\cdot G(\lambda_t)$ serves as an indicator of the current performance of the system, i.e., how far the system is from its objective. As mentioned above, there are two critical parameters that a designer can utilize: T which is the desired ratio between users and miners in the system, and parameter d which calibrates the intensity of the updates. We can simplify the above formula as:

$$\lambda_{t+1} = \lambda_t + \eta\lambda_t(1-\lambda_t)\cdot\left(\bar{F}(\lambda_t) - wG(\lambda_t)\right)$$

where $\eta = U\cdot d$ and $w = T\cdot\frac{M}{U}$. Finally, we can reformulate the above formula as

$$\lambda_{t+1} = \lambda_t + \eta\lambda_t(1-\lambda_t)\cdot\Delta_w(\lambda_t) \qquad \text{(MEV-D)}$$

where $\Delta_w(\lambda_t) := \bar{F}(\lambda_t) - wG(\lambda_t)$. The important design parameters in (MEV-D) are the adjustment quotient, η, and the target participation ratio, w. For our purposes, it will also be helpful to define the update function $h : [0,1] \to [0,1]$ as

$$h(\lambda) = \lambda + \eta\lambda(1-\lambda)\Delta_w(\lambda). \tag{1}$$

Whenever obvious, we will omit the dependence of $\Delta_w(\lambda)$ on w, and we will simply write $\Delta(\lambda)$ or $\Delta(\lambda_t)$ when time is relevant.

3 EVOLUTION OF THE DYNAMIC MEV EXTRACTION RATES

The analysis of the above dynamical system, defined by (MEV-D), will be our main focus. Our first observation is that under our working assumptions on F and G, the target function $\Delta(\lambda)$ satisfies some useful properties.

Property 1 (Properties of Target Function $\Delta(\lambda)$). *Let $w > 0$, and assume that F, G are differentiable and strictly increasing with support in $[0,1]$. Then, the function $\Delta(\lambda) := \bar{F}(\lambda) - wG(\lambda)$ satisfies the following properties:*

(i) $\Delta(\lambda)$ is strictly decreasing for $\lambda \in [0,1]$ with $\Delta(0) = 1$, and $\Delta(1) = -w$.
(ii) There exists a unique $\lambda^* \in (0,1)$ such that $\Delta(\lambda^*) = 0$.
(iii) There exists a function $K : [0,1] \to \mathbb{R}$ so that $\Delta(\lambda) = (\lambda - \lambda^*)\cdot K(\lambda)$, and $\lim_{x\to\lambda^*} K(x) < +\infty$.

Proof. Properties $(i), (ii)$ and the existence part of (iii) are straightforward and their proof is omitted. To see why the second part of (iii) holds, observe that since F, G are differentiable in $(0,1)$, de l'Hôpital's rule implies that

$$\begin{aligned}\lim_{\lambda\to\lambda^*} K(\lambda) &= \lim_{\lambda\to\lambda^*}\frac{\Delta(\lambda)}{\lambda-\lambda^*} = \lim_{\lambda\to\lambda^*}(-f(\lambda) - wg(\lambda))\\ &= -f(\lambda^*) - wg(\lambda^*) < +\infty\end{aligned}$$

which holds since the probability distribution functions exist and are continuous by assumption. □

Based on the above, our first observation is that, by construction, (MEV-D) has 3 fixed points. These are $\lambda = 0$, $\lambda = 1$ and a unique (under our assumptions) interior point $\lambda^* \in (0,1)$ such that $\Delta_w(\lambda^*) = 0$. The first two fixed points are considered *degenerate states* of the system: the former corresponds to no MEV extraction and, thus, miners are not willing to participate. The latter corresponds to a state in which MEV extraction rate is so high that no user is willing to interact with the blockchain.

We are primarily interested in analyzing the evolution of the dynamics with respect to the third fixed point, i.e., the unique interior fixed point which corresponds to the optimal state of the system, i.e., target levels of user/miner participation. Before we proceed with our results about the behavior of (MEV-D), we introduce a necessary definition.

Definition 3.1 (Directionally Stable Fixed Point). Let $\{\lambda_t\}_{t\geq 0}$ be a one-dimensional dynamical system determined by a function $h : \mathbb{R} \to \mathbb{R}$, so that $\lambda_{t+1} := h(\lambda_t)$, and let λ^* be a fixed point of h, i.e., $h(\lambda^*) = \lambda^*$. Then λ^* is called *directionally stable* for $\{h_t\}_{t\geq 0}$, if for every $t \geq 0$ such that $\lambda_t \neq \lambda^*$ it holds that $(h(\lambda_t) - \lambda_t)/(\lambda_t - \lambda^*) < 0$ where $h(\lambda_t) = \lambda_{t+1}$ for every $t \geq 0$.

In other words, if a fixed point is *directionally stable* then the dynamical system moves towards the direction of this fixed point at every iteration. We will now proceed to show that in (MEV-D), the fixed point $0 < \lambda^* < 1$ is *directionally stable.*

Lemma 3.2. *The unique interior fixed point, λ^* of the* (MEV-D) *is directionally stable, i.e., it holds that $h(\lambda) > \lambda$ whenever $0 < \lambda < \lambda^*$ and $h(\lambda) < \lambda$ whenever $\lambda^* < \lambda < 1$.*

Proof. First, for $\lambda > \lambda^*$ it holds that $\Delta_w(\lambda) < 0$ since $\Delta_w(\lambda^*) = 0$ and Δ_w is a decreasing function and hence $h(\lambda) - \lambda = \lambda(1-\lambda)\Delta_w(\lambda) < 0$. Thus, $(h(\lambda) - \lambda)/(\lambda - \lambda^*) < 0$. Similarly, for $\lambda < \lambda^*$ it holds that $\Delta_w(\lambda) > 0$ and subsequently $(h(\lambda) - \lambda)/(\lambda - \lambda^*) < 0$. This concludes the proof that λ^* is *directionally stable.* □

Directional stability secures that whenever a trajectory reaches a point close to a degenerate state, i.e., $\lambda = 0$ or $\lambda = 1$, the next step will move towards the fixed point λ^*. Due to the factors λ (resp. $(1-\lambda)$), the updates close to the boundaries will be small. This trend will continue until the trajectory reaches or overshoots the fixed point λ^*.

An important implication of the previous observation is that the system can reach the degenerate state $\lambda = 0$ at time $t+1$ only when $\lambda_t > \lambda^*$, and similarly, it can reach the degenerate state $\lambda = 1$ only when $\lambda_t < \lambda^*$. Further elaborating on this, we can derive a condition on the intensity of system updates, to ensure that these two boundary fixed points will *never* be reached by the dynamics, for any interior starting point, $\lambda_0 \in (0,1)$.

Theorem 3.3. *(Market-Liveness) For any pair of tolerance distributions, F, G, target w, and starting point $\lambda_0 \in (0,1)$, it holds that $\lambda_t \in (0,1)$ for any $t > 0$ as long as*

$$\eta < \min\left\{\frac{1}{w(1-\lambda^*)}, \frac{1}{\lambda^*}\right\}.$$

where λ^* is the unique solution of the equation $\Delta(\lambda) = 0$ in $(0,1)$.

Proof. We first consider the case of avoiding the fixed point at $\lambda = 0$. If $0 < \lambda_t < \lambda^*$ for some $t \geq 0$, then by Lemma 3.2, it holds that $\lambda_{t+1} = h(\lambda_t) > \lambda_t$ which implies, in particular, that $h(\lambda_t) \neq 0$. Thus, for the dynamics to reach 0, it must be the case that $\lambda_t > \lambda^*$ and $h(\lambda_t) \leq 0$ (recall that if $h(\lambda_t) < 0$, then the λ_{t+1} is projected

back to 0). To exclude this case, we need to ensure that $h(\lambda_t) > 0$ for all $\lambda > \lambda^*$ which can be written as

$$\Delta(\lambda) > \frac{-1}{\eta(1-\lambda)}, \quad \text{for all } 1 > \lambda > \lambda^*. \tag{2}$$

Since $\Delta(\lambda) = \bar{F}(\lambda) - wG(\lambda) > -w$, and $\frac{-1}{\eta(1-\lambda^*)} > \frac{-1}{\eta(1-\lambda)}$ for all $1 > \lambda > \lambda^*$, a sufficient condition for the inequality in (2) to hold is that $-w > \frac{-1}{\eta(1-\lambda^*)}$ or equivalently that $\eta < \frac{1}{w(1-\lambda^*)}$. The case of the fixed point at $\lambda = 1$ is similar. In particular, if $\lambda^* < \lambda_t < 1$ for some $t \geq 0$, then, by Lemma 3.2, the dynamics will decrease in the next step. Thus, the only case for (MEV-D) to reach 1 is that $\lambda_t < \lambda^*$ and $h(\lambda_t) \geq 1$. As before, to exclude this case, we need to ensure that $h(\lambda_t) < 1$ for all $0 < \lambda < \lambda^*$ which can be written as

$$\Delta(\lambda) < \frac{1}{\eta\lambda}, \quad \text{for all } 0 < \lambda < \lambda^*. \tag{3}$$

Since $\Delta(\lambda) = \bar{F}(\lambda) - wG(\lambda) < 1$, and $\frac{1}{\eta\lambda} > \frac{1}{\eta\lambda^*}$ for all $0 < \lambda < \lambda^*$, a sufficient condition for the inequality in (3) to hold is that $1 < \frac{1}{\eta\lambda^*}$ or equivalently that $\eta < \frac{1}{\lambda^*}$. Putting these two conditions together, we obtain the claim, namely that $\eta < \min\left\{\frac{1}{\lambda^*}, \frac{1}{w(1-\lambda^*)}\right\}$. □

Theorem 3.3 provides a sufficient condition for the values of the control parameter η for which (MEV-D) never reaches the degenerate states $\lambda \in \{0, 1\}$. We next turn our attention to the evolution of the system for lower values of η, i.e., for values of η below the upper bound of Theorem 3.3. As we show in Theorem 3.4, at the other extreme, i.e., for sufficiently low values of η, the (MEV-D) converge to the fixed point λ^*.

Theorem 3.4 (Lazy Updates - Convergence to λ^*). *For any pair of tolerance distributions, F, G, target w and starting point $\lambda_0 \in (0, 1)$, the sequence $\{\lambda_t\}_{t>0}$ generated by* (MEV-D) *converges to λ^*, for any control parameter $\eta > 0$ such that*

$$\eta \leq \inf_{\lambda \neq \lambda^*} \frac{(\lambda^* + \lambda)}{\lambda^2(1-\lambda)K(\lambda)}.$$

Proof. We will prove that the function $\Phi(\lambda) := (\ln\lambda - \ln\lambda^*)^2$ decreases along any trajectory of the dynamics, i.e., that $\Phi(h(\lambda)) < \Phi(\lambda)$ for any $\lambda \in (0, 1)$ with $\lambda \neq \lambda^*$. This is equivalent to showing that

$$(\ln h(\lambda) - \ln\lambda^*)^2 < (\ln\lambda - \ln\lambda^*)^2, \text{ for any } \lambda \neq \lambda^*. \tag{4}$$

In other words, we will show that $\Phi(\lambda)$ acts as a potential function for the (MEV-D) which directly implies convergence. To proceed, we rewrite the above inequality as $(\ln h(\lambda) - \ln\lambda^*)^2 - (\ln\lambda - \ln\lambda^*)^2 = (\ln h(\lambda) - \ln\lambda) \cdot (\ln h(\lambda) + \ln\lambda - 2\ln\lambda^*) = \ln\left(\frac{h(\lambda)}{\lambda}\right) \cdot \ln\left(\frac{\lambda h(\lambda)}{(\lambda^*)^2}\right)$. We will consider two cases, depending on whether $\lambda < \lambda^*$ or $\lambda > \lambda^*$:

- $\lambda < \lambda^*$: In this case, it holds that $h(\lambda) > \lambda$, see Definition 3.1 and Lemma 3.2, which implies that $h(\lambda)/\lambda > 1$. Hence, $\ln\left(\frac{h(\lambda)}{\lambda}\right) > 0$. Thus, to obtain the desired inequality, we need to select $\eta > 0$ so that the argument of the second ln on the right hand side of the above equation is less than 1, i.e., $\lambda h(\lambda)/(\lambda^*)^2 < 1$. Solving this inequality for η yields the inequality $\eta < \frac{(\lambda^*-\lambda)(\lambda^*+\lambda)}{\lambda^2(1-\lambda)\Delta(\lambda)}$, where we used that $\Delta(\lambda) > 0$ for all $\lambda < \lambda^*$. Since this inequality must hold for any $\lambda < \lambda^*$, we obtain the threshold $\eta \leq \inf_{\lambda<\lambda^*} \frac{(\lambda^*-\lambda)(\lambda^*+\lambda)}{\lambda^2(1-\lambda)\Delta(\lambda)}$. It remains to show that the threshold on the right hand side remains strictly positive for any distributions. Using Property 1, we can rewrite the threshold as $\inf_{\lambda<\lambda^*} \frac{\lambda^*+\lambda}{\lambda^2(1-\lambda)K(\lambda)}$. Since $\Delta(0) = 1$, it follows that $K(0) = 1/\lambda^*$ which implies that $\lim_{\lambda\to 0^+} \frac{\lambda^*+\lambda}{\lambda^2(1-\lambda)K(\lambda)} = +\infty$, and $\lim_{\lambda\to(\lambda^*)^-} \frac{\lambda^*+\lambda}{\lambda^2(1-\lambda)K(\lambda)} = \frac{2}{\lambda^*(1-\lambda^*)\cdot\lim_{\lambda\to(\lambda^*)^-} K(\lambda)}$. Thus, since $\lim_{\lambda\to(\lambda^*)^-} K(\lambda)$ exists and is less than $+\infty$ by Property 1, the claim follows.
- $\lambda > \lambda^*$: in this case, it holds that $h(\lambda) < \lambda$, see Definition 3.1 and Lemma 3.2, which implies that $h(\lambda)/\lambda < 1$. Hence, $\ln\left(\frac{h(\lambda)}{\lambda}\right) < 0$. Thus, to obtain the desired inequality in (4), we need to select $\eta > 0$ so that the argument of the second ln on the right hand side of the above equation is larger than 1, i.e., $\lambda h(\lambda)/(\lambda^*)^2 > 1$. Solving this inequality for η yields the same inequality as above (note that this time, $\Delta(\lambda) < 0$).

Putting the two cases together, we have that the (MEV-D) converge to λ^* whenever $0 < \eta \leq \inf_{\lambda\neq\lambda^*} \frac{(\lambda^*+\lambda)}{\lambda^2(1-\lambda)K(\lambda)}$ as claimed. □

Together with Theorem 3.3, Theorem 3.4 paints the picture for extreme values of update intensities, i.e., either sufficiently high (degenerate market), in which the system collapses by reaching either of the two boundary fixed points, or sufficiently low (lazy updates), in which case the system stabilizes to the unique optimal state. Intuitively, the sufficiency condition of Theorem 3.4 suggests that convergence to λ^* occurs when the intensity of the updates is small enough *in comparison* to current market conditions as these are captured by function $\Delta(\lambda)$, i.e., the distributions of users' and miners' tolerances. However, low values of the control parameter η correspond to a system with slow responses and come at the trade-off of slow responses to otherwise fast-changing market conditions. Thus, such values may be irrelevant for practical applications [36].

This leaves open the case in which this condition is not satisfied. Interestingly, as we show next, in this case, the system may exhibit arbitrarily complex behavior. Specifically, in Theorem 3.9, we prove that for any value of η, there exist distributions F, G, satisfying our assumptions, for which the system does not converge to λ^*. In particular, based on the aggressiveness of the updates, the system can become provably chaotic in the sense of *Li-Yorke chaos* [27]. Counterintuitively, as we show in Section 4, this chaotic behavior is not necessarily detrimental to system performance. Although chaotic updates in the MEV extraction rates make their evolution unpredictable, they keep the system non-degenerate, in the sense that they remain bounded away from 0 and 1, thus, ensuring participation of both users and miners. Before we proceed to prove that the (MEV-D) become Li-Yorke chaotic, we introduce new necessary notations and definitions. Our technical tools in this part extend the framework of [24].

Definition 3.5 (Periodic Orbit and Points). Consider a dynamical system, $(\lambda_t)_{t\geq 0}$, defined by a function $h : \mathbb{R} \to \mathbb{R}$ so that $\lambda_{t+1} = h(\lambda_t)$ for any $t \geq 0$. A sequence $\lambda_1, \lambda_2, \ldots, \lambda_k$ is called a *periodic orbit of length k* of the dynamical system, if $\lambda_{t+1} = h(\lambda_t)$ for $1 \leq i \leq k-1$ and $h(\lambda_k) = \lambda_1$. Each point $\lambda_1, \lambda_2, \ldots, \lambda_k$ is called periodic point of least period k.

Definition 3.6 (Li-York chaos [27]). Let $X = [L, U]$ be a compact interval in $\mathbb{R}$ and let $h : X \to X$ define a discrete-time dynamical system $(x_t)_{t\geq 0}$ on X, so that $x_t := h^t(x_0)$ for any $x_0 \in X$. The dynamical system $(x_t)_{t\in N}$ is called *Li-Yorke chaotic* if it holds that (1) For every $k = 1, 2, \dots$ there is a periodic point in X with period k. (2) There is an uncountable set $S \subseteq X$ (containing no periodic points), which satisfies the following conditions:

- For every $x \neq y \in S$, $\lim_{t\to\infty} \sup|h^t(x) - h^t(y)| > 0$ and $\lim_{t\to\infty} \inf |h^t(x) - h^t(y)| = 0$.
- For every points $x \in S$ and $y \in X$, $\lim_{t\to\infty} \sup|h^t(x) - h^t(y)| > 0$.

Famously, a sufficient condition for a system to be *Li-Yorke chaotic* is to have a period point of period of 3 [27]. This implication relies on the Sharkovsky Ordering and Sharkovsky's theorem which are presented next [39].

Definition 3.7 (Sharkovsky Ordering [4]). The following ordering of the set $\mathbb{N}$ of positive integers, is known as the Sharkovsky ordering: $3 > 5 > 7 > 9 > \cdots$, $3 \cdot 2 > 5 \cdot 2 > 7 \cdot 2 > 9 \cdot 2 > \cdots$, $3 \cdot 2^n > 5 \cdot 2^n > 7 \cdot 2^n > 9 \cdot 2^n > \cdots$, and $\cdots > 2^n > \cdots > 2^2 > 2 > 1$. This is a total ordering, i.e., every positive integer appears exactly once in the list.

Theorem 3.8 (Sharkovsky [39]). *Let $X \subset \mathbb{R}$ be a compact interval and let $h : X \to X$ be a continuous function. If h has a periodic point of least period m, then h has a periodic point of least period l for every l such that $m > l$ in the Sharkovsky ordering.*

Using these results, we will now formally prove that for every intensity, η, in the MEV extraction rate updates, there exist tolerance distributions F, G such that (MEV-D) become *Li-York chaotic*.

Theorem 3.9 (Chaotic Updates). *For every intensity level, $\eta > 0$, there exist continuous distributions F, G such that the* (MEV-D) *become Li-Yorke chaotic.*

Proof. The proof is constructive and proceeds by creating an instance for which the dynamics have a periodic point of least period 3. The instance depends on the η and thus, it can apply to any $\eta > 0$. Specifically, we consider a case in which both users and miners have the same tolerance distributions on $[a, b]$ with $0 < a < b <$. In this case, the update function (1) can be written as

$$h(\lambda) = \begin{cases} \lambda(-\eta\lambda + \eta + 1), & 0 \leq \lambda < a, \\ \lambda(-\eta\lambda\Delta(\lambda) + \eta\Delta(\lambda) + 1), & a \leq \lambda < b, , \\ \lambda(\eta w\lambda - \eta w + 1) & b \leq \lambda \leq 1, \end{cases}$$

with $\Delta(\lambda) := \frac{b+wa-\lambda(1+w)}{b-a}$. We will prove that for any fixed $\eta > 0$, there exist a, b such that the dynamical system has a periodic orbits of period 3. Since the update function, h is continuous, we will prove that by finding points $\lambda_0, \lambda_1, \lambda_2, \lambda_3$ such that

$$\lambda_1 = h(\lambda_0),\ \lambda_2 = h(\lambda_1) = h^2(\lambda_0),\ \lambda_3 = h(\lambda_2) = h^3(\lambda_0)$$

which satisfy $\lambda_3 \leq \lambda_0 < \lambda_1 < \lambda_2$. Firstly, for $0 \leq \lambda < a$, the update function h is increasing and $\lambda < h(\lambda)$. Thus, there exists $0 < \lambda_0 < a$ such that $h(\lambda_0) = a$. Let $\lambda_1 = a, \lambda_2 = h(a)$ and $\lambda_3 = h^2(a)$. Then, $h(a) = a+\eta a(1-a)$ and, hence, $a < h(a)$. Moreover $\Delta(h(a)) = 1-\eta c$, where $c = \frac{a(1-a)(1+w)}{b-a}$ and, as $b \to a^+$, $c \to \infty$. Lastly, we compute

$$h(h(a)) = h(a) + \eta h(a)(1 - h(a))\Delta(h(a)).$$

After some trivial algebra, we get that

$$h(h(a)) = -(h(a) - (h(a))^2)\eta^2 c + (h(a) - (h(a)^2))\eta + h(a).$$

We want to prove that $\lambda_3 = h(h(a)) \leq \lambda_0$ which is equivalent to

$$-(h(a) - (h(a))^2)\eta^2 c + (h(a) - (h(a)^2))\eta + h(a) \leq \lambda_0.$$

This is true as $b \to a^+$, since $h(a) - (h(a))^2 > 0$. Thus we get $\lambda_3 \leq \lambda_0 < \lambda_1 < \lambda_2$, which concludes the proof. □

Intuitively, the construction in the proof of Theorem 3.9 suggests that as the tolerance of users and/or miners becomes more concentrated around some value, then the dynamics are more likely to become chaotic since even small updates in the MEV extraction rate have significant impact in the participation rates of the system.

3.1 Visualizations

In order to gain a better intuition on the results of the previous section, in this part, we provide visualizations of the (MEV-D) that showcase the various cases discussed above.

To instantiate the dynamics, we select specific instances of Beta distributions for both users and miners because these distributions have the desirable properties that (1) their support range is $[0, 1]$, matching the values of possible MEV extraction tolerance for miners and users, and (2) they have the expressive capacity to capture many different forms of valuation distributions. The results for a specific instance are provided in the *bifurcation diagram* in Figure 1.

In the bifurcation diagram, the horizontal axis corresponds to values of the update instensity, η. It is straightforward to see, that for any fixed value of η, the (MEV-D) either converge (low values of η) or are restricted in a bounded area around λ^*. This bounded area expands as η increases till it reaches one of the boundaries (in this case $\lambda = 0$) which implies that the dynamics get trapped there (with dire implications for the two-sided market).

The instance depicted in the left panel of Figure 1 captures all cases described in our previous formal analysis. From Figure 1, we can also see some regimes, e.g., around $\eta \approx 0.4$, in which the dynamics only have *periodic orbits*. In fact, using Theorem 3.8, we can further argue about the behavior of the system in these cases.

3.1.1 Regions of Periodic Orbits. To better understand the orbits of Equation (MEV-D), we visualize the function $h^{(k)}(\lambda)$ and observe its fixed points, $\lambda = h^{(k)}(\lambda)$ for various values of $k \in \mathbb{N}$. In particular, Theorem 3.8 implies that if we can find $k \geq 2 \in \mathbb{N}$ such that the function $h(\lambda)$ has periodic points of least period k, but *not* of least period $k + 1$, then the dynamics generated by h have periodic orbits with all possible periods that precede k in the Sharkovsky ordering. As mentioned above, such regimes are visible around $\eta = 0.4$ in Figure 1.

In Figure 2, we visualize one such instance that corresponds to areas of periodic behavior for $\eta = 0.5$. Note that for η slightly larger than 0.6, the bifurcation diagram shows a range of parameter values for which apparently the only cycle has period 3. In fact, according to Theorem 3.8, there must be cycles of all periods there, but they are not stable and therefore not visible on the computer-generated simulation.

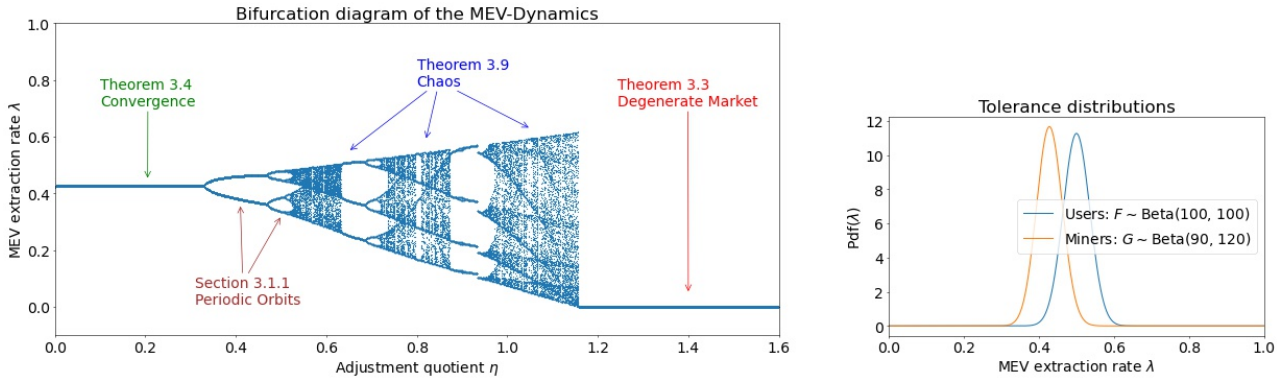

Figure 1: Bifurcation diagram for the (MEV-D) **with respect to the adjustment intensity η (left panel). The tolerance distributions of miners and users are shown in the panel on the right. For low values of η, the dynamics converge to λ^* (Theorem 3.4), whereas for large values of λ, the dynamics reach the boundary and get trapped at the corresponding fixed point (in this case 0) in which case, the two-sided market collapses (Theorem 3.3). For intermediate values of η, the dynamics are either provably chaotic (Theorem 3.9) or periodic with periods of difference density (Section 3.1.1).**

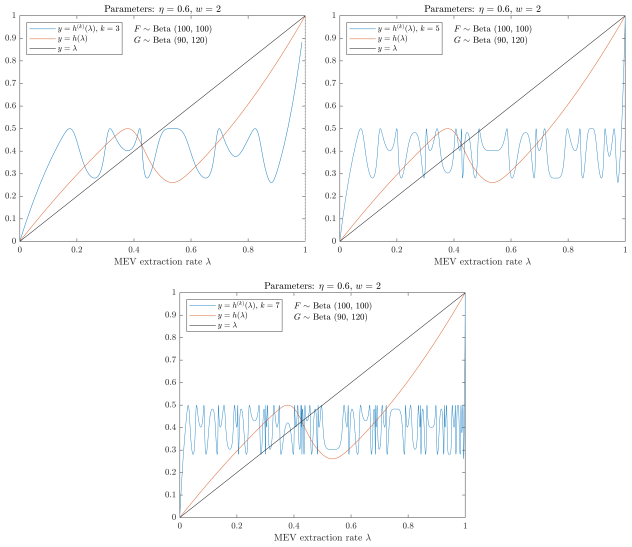

Figure 2: Regions of periodic behavior for the instance of Figure 1 and $\eta = 0.6$. The panels indicate the existence of periodic points of least period $k = 5$ and $k = 7$, but not of $k = 3$ (the period k is denoted in the legends). According to Theorem 3.8, this means that for these parameters, the (MEV-D) **have periodic points of uncountably many periods but are not provably chaotic. Similarly, we can create instances with periods of $k = 4, 2$ and 1 but not of $k = 8$ etc (see Appendix A).**

4 PERFORMANCE

In the previous section, we analyzed the long-term performance of (MEV-D). We studied three properties regarding the evolution of the system; conditions for convergence, conditions for not reaching the boundaries and conditions for chaotic behavior. Having established these, we now turn to the performance of the system in these regimes. As mentioned above, low values of the control parameter, η, allow the dynamics to stabilize at the fixed point λ^*. However, such values may lead to slow responses of the system against fast-changing market conditions and may be rarely applicable in practice. Moreover, the intensity of the updates is only relative to prevailing market conditions which may be subject to continuous changes.

Thus, the important question that we need to study is whether the system can exhibit desirable performance even when it is pushed beyond the stable regime, into the densely periodic or chaotic regimes. This is critical to ensure near-optimality, i.e., bounded deviations from target, long-term survival, i.e., market-liveness, and ultimately, persistence of the system under possibly adverse conditions. Interestingly, our analysis will not only establish such desirable behavior in out of equilibrium conditions, but also provide formal guarantess (rigorous proofs) that this will be the case.

4.1 Bounded Deviations and Average-Case Performance

Remember that, based on Sharkovsky's Theorem (Theorem 3.8) the further left a period point of m is in the Sharkovsky's ordering (Definition 3.7), the denser the periodic orbits are. Thus, to measure the performance of this system, we study if the target ratio w is achieved on average, or equivalently the time-average behavior of the values of the target function, i.e., $\lim_{T\to\infty} \frac{1}{T} \sum_{t=1}^{T} \Delta(\lambda)$.

In Figure 3, we visualize the values of $\Delta(\lambda_t)$ for the instance of Figure 1. As the control parameter η increases, the average deviations increase. This trend (deviation from average optimal performance) continues until the dynamics hit the boundary leading to non-liveness. The simulations suggest that optimal values the control parameter η, as far as achieving the target w on average is concerned, correspond to regimes with chaotic or complex - periodic with dense periods - evolution of the MEV extraction rate. From a practical perspective, such regimes ensure *market-liveness* along with bounded deviations from the target (see Lemma 4.1).

In the remainder of this section, we quantify these empirical results regarding system performance. Our first observation is that

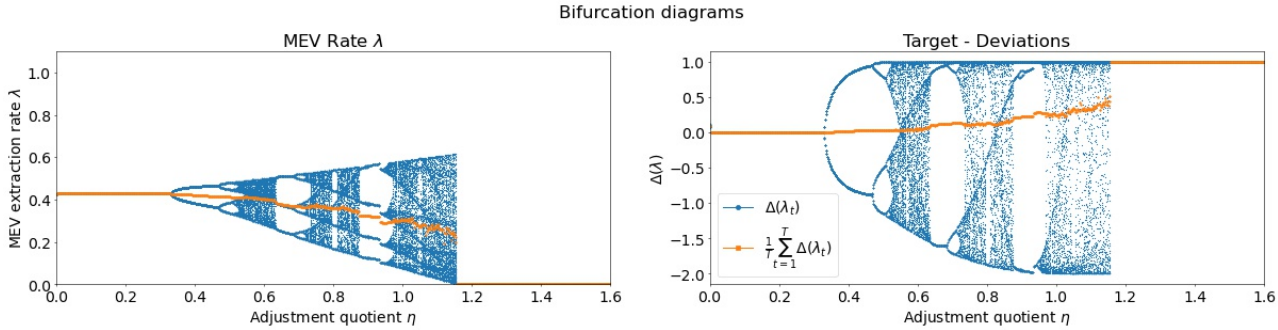

Figure 3: Performance of the (MEV-D) **in the instance of Figure 1, cf. left panels in both Figures. The simulations use a burn-in period of** 200 **iterations followed by** $T = 200$ **iterations that are plotted in the bifuraction diagrams. The right panel shows the values of the target,** $\Delta(\lambda_t)$**, for each** $t = 201, \ldots, 400$ **in blue dots and the averages over this period in light-colored dots (see also the legend). As** η **grows, the deviations from the target also grow till the dynamics hit the boundary and get absorbed there.**

the sequence of MEV extraction rates, $(\lambda_t)_{t\geq 0}$, remains within a bounded neighborhood of λ^*, which depending on the size of η, can be non-trivial (i.e., strictly between 0 and 1) even in the chaotic or densely-periodic cases. This is formally stated in Lemma 4.1.

Lemma 4.1 (Attracting range of λ.). *Consider an instance of the* (MEV-D) *with* $\eta, w > 0$ *and tolerance distributions* F, G *with* $\lambda^* \in (0,1)$ *such that* $\Delta(\lambda^*) = 0$ *as usual. Then, for the sequence of MEV extraction rates* $(\lambda_t)_{t\geq 0}$ *generated by the* (MEV-D) *it holds that*

$$\max\left\{0, \lambda^* - \frac{w\eta}{4}\right\} \leq \lambda_t \leq \min\left\{\lambda^* + \frac{\eta}{4}, 1\right\} \text{ for all } t \geq 0.$$

Proof. By Lemma 3.2, we know that $h(\lambda) > \lambda$ only if $\lambda < \lambda^*$. Thus, $h(\lambda) = \lambda + \eta\lambda(1-\lambda)\Delta(\lambda) < \lambda^* + \eta \cdot \frac{1}{4} \cdot 1 = \lambda^* + \frac{\eta}{4}$, where we used that $\Delta(\lambda) \leq 1$ for all $\lambda \in [0,1]$. Similarly, to determine the lower bound, we need to consider $\lambda > \lambda^*$. In this case, we have that

$$h(\lambda) = \lambda + \eta\lambda(1-\lambda)\Delta(\lambda) > \lambda^* + \eta\lambda(1-\lambda)\cdot(-w) > \lambda^* - \frac{\eta w}{4},$$

where we used that $\Delta(\lambda) \geq -w$ for all $\lambda \in [0,1]$. □

Note that the conditions $\lambda^* - \frac{w\eta}{4} > 0$ whenever $\eta < \frac{4\lambda^*}{w}$ and $\lambda^* + \frac{\eta}{4} < 1$ whenever $\eta < 4(1-\lambda^*)$. By Lemma 4.1, these inequalities offer an alternative set of market-liveness conditions to those of Theorem 3.3.

The result of Lemma 4.1 is practically relevant when η is small enough, so that both comparisons are resolved with the non-trivial bounds, rather than with 0 and 1. For such values of η, the sequence λ_t remains bounded between $\lambda^* - \frac{w\eta}{4}$ and $\lambda^* + \frac{\eta}{4}$. This allows us to bound the possible values of $\Delta(\lambda_t)$, i.e., the possible deviations from the target $\Delta(\lambda^*) = 0$. To do so, we proceed with a concrete expression for function $\Delta(\lambda)$ that uses the class of beta distributions for the tolerances of both miners and users.[7] The result regarding performance is provided in Theorem 4.2.

Theorem 4.2 (Bounded Deviations). *Consider an instance of the* (MEV-D) *with* $F \sim Beta(a,b), G \sim Beta(c,d)$ *and* η, w *such that* $0 < \lambda^* - \frac{w\eta}{4} < \lambda^* + \frac{\eta}{4} < 1$. *Then, we have*

$$|\Delta(\lambda_t)| \leq \frac{\eta(1+w)}{4}\left(\max_{\lambda\in(p,q)}\{f(\lambda)\} + w\max_{\lambda\in(p,q)}\{g(\lambda)\}\right),$$

where f, g *denote the probability density functions of* F, G *and* $p = \lambda^* - \frac{w\eta}{4}, q = \lambda^* + \frac{\eta}{4}$.

Proof. Since $\Delta(\lambda_t)$ is decreasing, we have by Lemma 4.1 that

$$\Delta\left(\lambda^* - \frac{w\eta}{4}\right) \geq \Delta(\lambda_t) \geq \Delta\left(\lambda^* + \frac{\eta}{4}\right),$$

for all λ_t's that lie in the attracting region of the dynamics, i.e., in $[\lambda^* - \frac{w\eta}{4}, \lambda^* + \frac{\eta}{4}]$ provided that η is such that $0 < \lambda^* - \frac{w\eta}{4}, \lambda^* + \frac{\eta}{4} < 1$. This implies that

$$\begin{aligned}|\Delta(\lambda_t)| &\leq \max\left\{\left|\Delta\left(\lambda^* - \frac{w\eta}{4}\right)\right|, \left|\Delta\left(\lambda^* + \frac{\eta}{4}\right)\right|\right\} \\ &\leq \left|\Delta\left(\lambda^* - \frac{w\eta}{4}\right)\right| + \left|\Delta\left(\lambda^* + \frac{\eta}{4}\right)\right|.\end{aligned}$$

Using the Mean Value Theorem, and the fact that $\Delta(\lambda^*) = 0$, we have that

$$\Delta\left(\lambda^* - \frac{w\eta}{4}\right) = \Delta\left(\lambda^* - \frac{w\eta}{4}\right) - \Delta(\lambda^*) = -\Delta'(x_1)\cdot\frac{w\eta}{4},$$

for some $x_1 \in \left(\lambda^* - \frac{w\eta}{4}, \lambda^*\right)$, and similarly that $\Delta\left(\lambda^* + \frac{\eta}{4}\right) = \Delta\left(\lambda^* + \frac{\eta}{4}\right) - \Delta(\lambda^*) = \Delta'(x_2)\cdot\frac{\eta}{4}$, for some $x_2 \in \left(\lambda^*, \lambda^* + \frac{\eta}{4}\right)$. Thus, to obtain meaningful bounds for $\Delta(\lambda_t)$, it suffices to bound the derivative of the function $\Delta(\lambda_t)$ for λ_t in the specified regions around λ^*. It holds that

$$\begin{aligned}|\Delta'(x)| &= |\bar{F}'(x) - wG'(x)| = |-f(x) - wg(x)| \\ &\leq \frac{1}{B(a,b)}x^{a-1}(1-x)^{b-1} + \frac{w}{B(c,d)}x^{c-1}(1-x)^{d-1} = H(x).\end{aligned}$$

Note that all coefficients in this expression are positive. Thus, we can complete the proof since

$$\begin{aligned}|\Delta(\lambda_t)| &\leq \left|\Delta\left(\lambda^* - \frac{w\eta}{4}\right)\right| + \left|\Delta\left(\lambda^* + \frac{\eta}{4}\right)\right| \\ &\leq \frac{\eta w}{4}\cdot\max_{x\in(p,\lambda^*)}\{H(x)\} + \frac{\eta}{4}\cdot\max_{x\in(\lambda^*,q)}\{H(x)\} \\ &\leq \frac{\eta(1+w)}{4}\cdot\max_{x\in(p,q)}\{H(x)\}\end{aligned}$$

[7] As mentioned above, beta distributions have the desirable properties that (1) their support range is $[0,1]$, matching the values of possible MEV extraction tolerance for miners and users, and (2) they have the expressive capacity to capture many different forms of valuation distributions.

which is less or equal than

$$\frac{\eta(1+w)}{4}\cdot\left(\frac{1}{B(a,b)}\cdot\max_{x\in(p,q)}\{x^{a-1}(1-x)^{b-1}\}+\frac{w}{B(c,d)}\cdot\max_{x\in(p,q)}\{x^{c-1}(1-x)^{d-1}\}\right)$$

as claimed. □

The next Lemma offers an exhaustive case analysis for the maximization problems that are involved in Theorem 4.2. Our intention is to use this lemma for values of $p=\lambda^*-\frac{w\eta}{4}$ and $q=\lambda^*+\frac{\eta}{4}$, to find analytically the maxima of the probability density functions f and g of the beta distributions as used in Theorem 4.2.

Lemma 4.3 (Maxima of Beta distributions). *Let $p,q\in(0,1)$ and $p<q$. Suppose that we are given a function $f:[0,1]\to\mathcal{R}$, such that $f(x)=x^{a-1}\cdot(1-x)^{b-1}$, for some fixed constant values $a,b\in\mathcal{R}$, and for any $x\in[0,1]$. Then we have the following: Suppose first that $a+b\neq 2$.*

- *If $2>a+b$ and*
  - *$\frac{1-a}{2-a-b}<p$, then f has the maximum value in $[p,q]$ that is $f(q)$; i.e. $\forall x\in[p,q]: f(x)\in(0,f(q)]$.*
  - *$p\leq\frac{1-a}{2-a-b}\leq q$, then f has the maximum value in $[p,q]$ that is $\tau=\max\{f(p),f(q)\}$; i.e. $\forall x\in[p,q]: f(x)\in(0,\tau]$.*
  - *$\frac{1-a}{2-a-b}>q$, then f has the maximum value in $[p,q]$ that is $f(p)$; i.e. $\forall x\in[p,q]: f(x)\in(0,f(p)]$.*
- *If $2<a+b$ and*
  - *$\frac{1-a}{2-a-b}<p$, then f has the maximum value in $[p,q]$ that is $f(p)$; i.e. $\forall x\in[p,q]: f(x)\in(0,f(p)]$.*
  - *$p\leq\frac{1-a}{2-a-b}\leq q$, then f has the maximum value in $[p,q]$ that is $\gamma=f\left(\frac{1-a}{2-a-b}\right)$; i.e. $\forall x\in[p,q]: f(x)\in(0,\gamma]$.*
  - *$\frac{1-a}{2-a-b}>q$, then f has the maximum value in $[p,q]$ that is $f(q)$; i.e. $\forall x\in[p,q]: f(x)\in(0,f(q)]$.*

If $a+b=2$, then under $a>1$, function f reaches it maximum at $x=q$, i.e., $\forall x\in[p,q]: f(x)\in(0,f(q)]$.

If $a+b=2$ and $a<1$, then function f reaches it maximum at $x=p$, i.e., $\forall x\in[p,q]: f(x)\in(0,f(p)]$.

Finally, if $a+b=2$ and $a=1$, then $f(x)=1$ for all $x\in[p,q]$.

Proof. Let us first observe that $f(x)>0$ for all $x\in[p,q]$. We have that

$$\begin{aligned}f'(x)&=(a-1)x^{a-2}(1-x)^{b-1}-x^{a-1}(b-1)(1-x)^{b-2}\\&=x^{a-2}(1-x)^{b-2}((2-a-b)x+a-1).\end{aligned}$$

We will now inspect the behavior of function f for $x\in[p,q]\subset(0,1)$. Then, because $x^{a-2}(1-x)^{b-2}>0$, unless $x\in\{0,1\}$, the monotonicity of f is determined by the sign of the linear function $(2-a-b)x+a-1$ of x.

Suppose first that $a+b\neq 2$, then $f'(\zeta)=0$ for $\zeta=\frac{1-a}{2-a-b}$. If $a+b<2$, then the function $(2-a-b)x+a-1$ of x is strictly increasing and its zero is ζ. This implies that $(2-a-b)x+a-1<0$ for $x<\zeta$ and $(2-a-b)x+a-1>0$ for $x>\zeta$. So function f is strictly decreasing when $x<\zeta$ and strictly increasing when $x>\zeta$, achieving its minimum at $x=\zeta$.

We now consider the following cases:

- $\zeta<p$: in this case function f in increasing when $x\in[p,q]$, meaning that it reaches its maximum at $x=q$
- $p\leq\zeta\leq q$: in this case function f in decreasing when $x\in[p,\zeta]$, and increasing when $x\in[\zeta,q]$, meaning that it reaches its maximum at $x=p$ or $x=q$, depending which of the two values $f(p)$, $f(q)$ is larger.
- $\zeta>q$: in this case function f in decreasing when $x\in[p,q]$, meaning that it reaches its maximum at $x=p$.

If $a+b>2$, then the function $(2-a-b)x+a-1$ of x is strictly decreasing, that is, $(2-a-b)x+a-1>0$ for $x<\zeta$ and $(2-a-b)x+a-1<0$ for $x>\zeta$. Thus, function f is strictly increasing when $x<\zeta$ and strictly decreasing when $x<\zeta$, achieving its maximum at $x=\zeta$.

We now consider the following cases:

- $\zeta<p$: in this case function f in decreasing when $x\in[p,q]$, meaning that it reaches its maximum at $x=p$.
- $p\leq\zeta\leq q$: in this case function f in increasing when $x\in[p,\zeta]$, and decreasing when $x\in[\zeta,q]$, meaning that it reaches its maximum at $x=\zeta$.
- $\zeta>q$: in this case function f in increasing when $x\in[p,q]$, meaning that it reaches its maximum at $x=q$.

Let us finally consider the case when $a+b=2$. Then $f'(x)=x^{a-2}(1-x)^{b-2}(a-1)>0$, when $a>1$ and $f'(x)<0$ when $a<1$. In the former case, function f is strictly increasing for $x\in[p,q]$ and therefore reaches it maximum at $x=q$. In the latter case, function f is strictly decreasing for $x\in[p,q]$ and therefore reaches it maximum at $x=p$. Finally, if $a+b=2$ and $a=1$, then $b=1$, therefore function f is a constant function $f(x)=1$ for all x. □

5 CONCLUSION

Maximal Extractable Value constitutes a critical issue in smart-contract blockchains. With the evolution of the MEV ecosystem, the whole process of extracting excess value from the economic activity of users has been systematized and benefits different kind of blockchain participants including searchers, builders, validators and block proposers. This creates a fundamental trade-off between users' sovereignty over their own transactions and revenue maximization for the entities who secure and process these transactions. Accordingly, a lot of research is concentrated on designing mechanisms that will return to users part of the excess value created by their economic activity.

Our work establishes the first to our knowledge dynamic framework for the integral problem of MEV sharing. Without arguing on whether MEV is desirable or not, this framework treats MEV as an unavoidable phenomenon of current blockchains and enables the market to decide dynamically on its exact level through a protocol-based implementation. Using the design principles of the EIP-1559 upgrade, our rigorous mathematical results provide the first formal evidence that similar mechanisms with properly engineered target functions can be successful in tackling blockchain optimization problems that extend beyond the current use of EIP-1559 in regulating transaction fee markets. From a practical perspective, our results suggest that dynamic MEV extraction can achieve targets set by the protocol and can, thus, inform the ongoing discussion about actively enshrining MEV extraction in protocol designs.

REFERENCES

[1] A. Ang and A. Timmermann. 2012. Regime Changes and Financial Markets. *Annual Review of Financial Economics* 4, 1 (2012), 313–337. https://doi.org/10.1146/annurev-financial-110311-101808 arXiv:https://doi.org/10.1146/annurev-financial-110311-101808

[2] K. Babel, P. Daian, M. Kelkar, and A. Juels. 2023. Clockwork Finance: Automated Analysis of Economic Security in Smart Contracts. In *2023 IEEE Symposium on Security and Privacy (SP)*. IEEE Computer Society, Los Alamitos, CA, USA, 2499–2516. https://doi.org/10.1109/SP46215.2023.10179346

[3] M. Bartoletti, J.H-y. Chiang, and A. Lluch Lafuente. 2022. Maximizing Extractable Value from Automated Market Makers. In *Financial Cryptography and Data Security*, I. Eyal and J. Garay (Eds.). Springer International Publishing, Cham, 3–19. https://doi.org/10.1007/978-3-031-18283-9_1

[4] K. Burns and B. Hasselblatt. 2011. The Sharkovsky Theorem: A Natural Direct Proof. *The American Mathematical Monthly* 118, 3 (2011), pp. 229–244. https://doi.org/10.4169/amer.math.monthly.118.03.229

[5] V. Buterin, E. Conner, R. Dudley, M. Slipper, I. Norder, and A. Bakhta. 2019. EIP-1559: Fee market change for ETH 1.0 chain. Published online: https://eips.ethereum.org/EIPS/eip-1559.

[6] Y.K. Cheung, S. Leonardos, and G. Piliouras. 2021. Learning in Markets: Greed Leads to Chaos but Following the Price is Right. In *Proceedings of the Thirtieth International Joint Conference on Artificial Intelligence, IJCAI-21*, Zhi-Hua Zhou (Ed.). International Joint Conferences on Artificial Intelligence Organization, Montreal, Canada, 111–117. https://doi.org/10.24963/ijcai.2021/16 Main Track.

[7] T. Chitra and K. Kulkarni. 2022. Improving Proof of Stake Economic Security via MEV Redistribution. In *Proceedings of the 2022 ACM CCS Workshop on Decentralized Finance and Security* (Los Angeles, CA, USA) *(DeFi'22)*. Association for Computing Machinery, New York, NY, USA, 1–7. https://doi.org/10.1145/3560832.3564259

[8] P. Daian, S. Goldfeder, T. Kell, Yunqi Li, X. Zhao, I. Bentov, L. Breidenbach, and A. Juels. 2020. Flash Boys 2.0: Frontrunning in Decentralized Exchanges, Miner Extractable Value, and Consensus Instability. In *2020 IEEE Symposium on Security and Privacy (SP)*. IEEE, San Francisco, CA, USA, 910–927. https://doi.org/10.1109/SP40000.2020.00040

[9] I. Diakonikolas, C. Papadimitriou, G. Pierrakos, and Y. Singer. 2012. Efficiency-Revenue Trade-Offs in Auctions. In *Automata, Languages, and Programming*, A. Czumaj, K. Mehlhorn, A. Pitts, and R. Wattenhofer (Eds.). Springer, Berlin, Heidelberg, 488–499. https://doi.org/10.1007/978-3-642-31585-5_44

[10] Flashbots. 2022. MEV-Boost. https://boost.flashbots.net/

[11] Flashbots. 2022. The Future of MEV is SUAVE. https://writings.flashbots.net/the-future-of-mev-is-suave/

[12] Flashbots. 2023. MEV-Explore. https://explore.flashbots.net/

[13] Flashbots. 2023. MEV-Share: programmably private orderflow to share MEV with users. https://collective.flashbots.net.

[14] Ethereum Foundation. 2023. Maximal Extractable Value (MEV). https://ethereum.org/en/developers/docs/mev/

[15] T. Galla and J.D. Farmer. 2013. Complex dynamics in learning complicated games. *Proceedings of the National Academy of Sciences* 110, 4 (2013), 1232–1236. https://doi.org/10.1073/pnas.1109672110 arXiv:https://www.pnas.org/doi/pdf/10.1073/pnas.1109672110

[16] L.M. Goodman. 2014. Tezos—a self-amending crypto-ledger White paper. https://tezos.com/whitepaper.pdf

[17] L. Heimbach and R. Wattenhofer. 2022. Eliminating Sandwich Attacks with the Help of Game Theory. In *Proceedings of the 2022 ACM on Asia Conference on Computer and Communications Security* (Nagasaki, Japan) *(ASIA CCS '22)*. Association for Computing Machinery, New York, NY, USA, 153–167. https://doi.org/10.1145/3488932.3517390

[18] H.-T. Kao, T. Chitra, R. Chiang, J. Morrow, and Gauntlet. 2020. An Analysis of the Market Risk to Participants in the Compound Protocol. In *Third International Symposium on Foundations and Applications of Blockchain (FAB '20)*. Schloss Dagstuhl, Santa Cruz, California, USA, online. https://scfab.github.io/2020/FAB2020_p5.pdf

[19] M. Kelkar, S. Deb, and S. Kannan. 2022. Order-Fair Consensus in the Permissionless Setting. In *Proceedings of the 9th ACM on ASIA Public-Key Cryptography Workshop* (Nagasaki, Japan) *(APKC '22)*. Association for Computing Machinery, New York, NY, USA, 3–14. https://doi.org/10.1145/3494105.3526239

[20] M. Kelkar, S. Deb, S. Long, A. Juels, and S. Kannan. 2021. Themis: Fast, Strong Order-Fairness in Byzantine Consensus. Cryptology ePrint Archive, Paper 2021/1465. https://eprint.iacr.org/2021/1465

[21] M. Kelkar, F. Zhang, S. Goldfeder, and A. Juels. 2020. Order-Fairness for Byzantine Consensus. In *Advances in Cryptology – CRYPTO 2020: 40th Annual International Cryptology Conference, CRYPTO 2020, Santa Barbara, CA, USA, August 17–21, 2020, Proceedings, Part III* (Santa Barbara, CA, USA). Springer-Verlag, Berlin, Heidelberg, 451–480. https://doi.org/10.1007/978-3-030-56877-1_16

[22] A. Kiayias, A. Russell, B. David, and R. Oliynykov. 2017. Ouroboros: A Provably Secure Proof-of-Stake Blockchain Protocol. In *Advances in Cryptology – CRYPTO 2017*, Jonathan Katz and Hovav Shacham (Eds.). Springer International Publishing, Cham, 357–388.

[23] K. Kulkarni, T. Diamandis, and T. Chitra. 2023. Towards a Theory of Maximal Extractable Value I: Constant Function Market Makers. arXiv:2207.11835 [cs.GT]

[24] S. Leonardos, B. Monnot, D. Reijsbergen, S. Skoulakis, and G. Piliouras. 2021. Dynamical Analysis of the EIP-1559 Ethereum Fee Market. In *Proceedings of the 3rd ACM Conference on Advances in Financial Technologies* (Arlington, Virginia) *(AFT '21)*. Association for Computing Machinery, New York, NY, USA, 114–126. https://doi.org/10.1145/3479722.3480993

[25] S. Leonardos, D. Reijsbergen, B. Monnot, and G. Piliouras. 2022. Optimality Despite Chaos in Fee Markets. Financial Cryptography and Data Secutiry '23, Springer International Publishing. https://fc23.ifca.ai/preproceedings/127.pdf

[26] S. Leonardos, D. Reijsbergen, and G. Piliouras. 2019. PREStO: A Systematic Framework for Blockchain Consensus Protocols. *IEEE Transactions on Engineering Management* 67 (2019), 1028–1044. https://api.semanticscholar.org/CorpusID:189928091

[27] T.-Y. Li and J. A. Yorke. 1975. Period Three Implies Chaos. *The American Mathematical Monthly* 82, 10 (1975), 985–992. https://doi.org/10.2307/2318254

[28] A. Likhodedov and T. Sandholm. 2004. Mechanism for Optimally Trading Off Revenue and Efficiency in Multi-unit Auctions. In *Agent-Mediated Electronic Commerce V. Designing Mechanisms and Systems*, P. Faratin, D. C. Parkes, J. A. Rodríguez-Aguilar, and W. E. Walsh (Eds.). Springer Berlin Heidelberg, Berlin, Heidelberg, 92–108. https://doi.org/10.1007/978-3-540-25947-3_6

[29] B. Monnot. 2022. Notes on Proposer-Builder Separation (PBS). https://barnabe.substack.com/p/pbs.

[30] B. Monnot. 2022. Unbundling PBS: Towards protocol-enforced proposer commitments (PEPC). https://ethresear.ch/t/unbundling-pbs-towards-protocol-enforced-proposer-commitments-pepc/13879?u=barnabe

[31] A. Obadia, A. Salles, L. Sankar, T. Chitra, V. Chellani, and P. Daian. 2021. Unity is Strength: A Formalization of Cross-Domain Maximal Extractable Value. arXiv:2112.01472 [cs.CR]

[32] G. Piliouras and J.S. Shamma. 2014. Optimization despite Chaos: Convex Relaxations to Complex Limit Sets via Poincaré Recurrence. In *Proceedings of the Twenty-Fifth Annual ACM-SIAM Symposium on Discrete Algorithms* (Portland, Oregon) *(SODA '14)*. Society for Industrial and Applied Mathematics, USA, 861–873.

[33] G. Piliouras and F-Y. Yu. 2023. Multi-Agent Performative Prediction: From Global Stability and Optimality to Chaos. In *Proceedings of the 24th ACM Conference on Economics and Computation* (London, United Kingdom) *(EC '23)*. Association for Computing Machinery, New York, NY, USA, 1047–1074. https://doi.org/10.1145/3580507.3597759

[34] K. Qin, L. Zhou, P. Gamito, P. Jovanovic, and A. Gervais. 2021. An Empirical Study of DeFi Liquidations: Incentives, Risks, and Instabilities. In *Proceedings of the 21st ACM Internet Measurement Conference* (Virtual Event) *(IMC '21)*. Association for Computing Machinery, New York, NY, USA, 336–350. https://doi.org/10.1145/3487552.3487811

[35] K. Qin, L. Zhou, and A. Gervais. 2022. Quantifying Blockchain Extractable Value: How dark is the forest?. In *2022 IEEE Symposium on Security and Privacy (SP)*. IEEE Computer Society, Los Alamitos, CA, USA, 198–214. https://doi.org/10.1109/SP46214.2022.9833734

[36] D. Reijsbergen, S. Sridhar, B. Monnot, S. Leonardos, S. Skoulakis, and G. Piliouras. 2021. Transaction Fees on a Honeymoon: Ethereum's EIP-1559 One Month Later. In *2021 IEEE International Conference on Blockchain (Blockchain)*. IEEE Computer Society, Los Alamitos, CA, USA, 196–204. https://doi.org/10.1109/Blockchain53845.2021.00034

[37] T. Roughgarden. 2020. Transaction Fee Mechanism Design for the Ethereum Blockchain: An Economic Analysis of EIP-1559. arXiv:2012.00854 [cs.GT]

[38] T. Roughgarden. 2021. Transaction Fee Mechanism Design. In *Proceedings of the 22nd ACM Conference on Economics and Computation* (Budapest, Hungary) *(EC '21)*. Association for Computing Machinery, New York, NY, USA, 792. https://doi.org/10.1145/3465456.3467591

[39] A. N. Sharkovsky. 1964. Coexistence of Cycles of Continuous Mapping of the Line into Itself. *Ukrainian Mathematical Journal* 16 (1964), 61–71.

[40] V.Buterin. 2013. Ethereum: A Next-Generation Smart Contract and Decentralized Application Platform. https://ethereum.org/669c9e2e2027310b6b3cdce6e1c52962/Ethereum_Whitepaper_-_Buterin_2014.pdf

[41] S. Werner, D. Perez, L. Gudgeon, A. Klages-Mundt, D. Harz, and W. Knottenbelt. 2023. SoK: Decentralized Finance (DeFi). In *Proceedings of the 4th ACM Conference on Advances in Financial Technologies* (Cambridge, MA, USA) *(AFT '22)*. Association for Computing Machinery, New York, NY, USA, 30–46. https://doi.org/10.1145/3558535.3559780

A APPENDIX: ROBUSTNESS OF FINDINGS - SIMULATIONS

In this section, we provide further simulations to test the robustness of our model. We remind that in the theoretical part, for our analysis, we considered stationary tolerance distributions for users and miners. However, a shift in the prevailing market conditions, dynamics, or dominant trends is a well studied phenomenon in finance and it is called regime changes [1]. In financial markets, a regime change refers to a transition from one market regime to another, characterized by distinct behavior and patterns. Regime changes can have a profound impact on various aspects of financial markets, including asset prices, volatility, investor sentiment, and trading strategies.

In Figure 4, we examine a realistic scenario with two market regimes. We envision an environment where there are two pairs of tolerance distributions F_1, G_1 and F_2, G_2. The transition between these two regimes is governed by a threshold of the MEV extraction rate (set at $\theta = 0.408$ in the experiments). When the MEV extraction rate is below (above) θ users and miners are in regime 1 (2). Building on this idea, we also adopt two different intensity values, η_1, η_2, for the updates based on the MEV extraction rate, and two target values w_1 and w_2. It is known that MEV extracted differs from one application to another. For instance, the MEV generated in decentralized exchanges is regular, whereas liquidations and NFT generate spikes of MEV. Thus, when a spike in MEV is observed, the updates must be more aggressive in order to restore the equilibrium or return to the bounded regions faster. In this scenario, we observe the evolution of (MEV-D) for 5,000 iterations. Initially the control parameter is set at $\eta_1 = 0.9$ and the target at $w_1 = 1.1$. If at a given time t the extraction rate becomes larger than the threshold, i.e., $\lambda_t > \theta$, this triggers a change in the control parameter to $\eta_2 = 1.0$ to deal with the new regime. Vice versa, when the (MEV-D) undershoots the threshold, the control parameter sets back to η_1.

We observe here that the extraction rate stabilizes and in fact it stabilizes within one of the two regimes – see Figure 4 (left). We also see quite good stabilisation of the target values in the right part of the figure. This experiment suggests that our model shows reasonable stability even when the market conditions change between two regimes.

Now, in the second scenario, Figure 5, we consider a very adversarial setting. This setting is akin to stress tests used by regulators and financial institutions in classical financial markets. In this setting, we split the evolution of (MEV-D) in 100 epochs, where each epoch consists of 50 consecutive blocks. In each epoch, we sample randomly a control parameter η from the interval $[0.4, 1]$ and target w from the interval $[0.5, 2]$. This simulates very drastic changes in the parameter η and w – see the yellow and green graphs in Figure 5. Moreover, every 10 blocks, we also perturb the tolerance (beta) distributions F, G by changing their respective parameters a_u, b_u and a_m, b_m. This perturbation emulates the (high) volatility in demand that may characterise financial markets in certain periods.

Even in this extreme stress test, the results support our theoretical findings. The market remains in a safe zone, in the sense that the system keeps fluctuating and is bounded around the respective target – see the top blue chart in Figure 5. As it is shown in Lemma 4.1, the bounded area expands as the control parameter η increases. This is evident also in this simulation if we compare the evolution of (MEV-D) with the trajectory of the random values drawn of the control parameter η. The evolution of the target value (bottom right pink diagram in Figure 5) exhibits a more challenging behavior, which on one hand shows how demanding our stress test is whilst on the other supports the need to investigate more dynamic environments.

Finally, Figure 6 complements the findings of Figure 2 with a different instance of η which only exhibits periods of $k = 4, 2$ and 1.

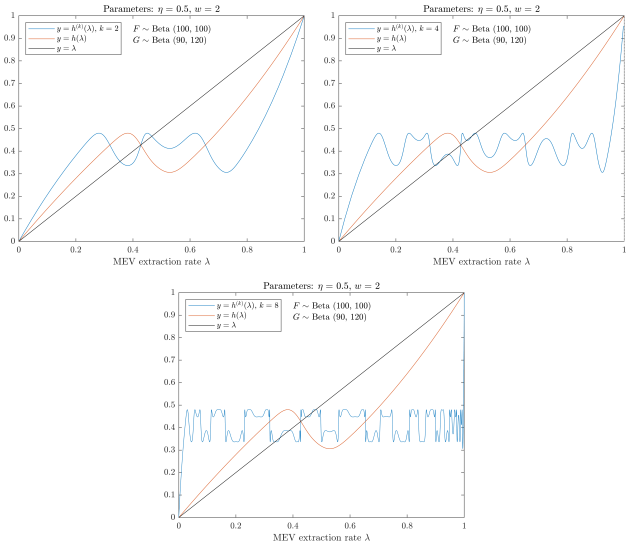

Figure 6: Regions of periodic behavior for the instance of Figure 1 for $\eta = 0.5$. In this case, there exist periodic points of least period $k = 2$ (left panel), periodic points of least period $k = 4$ (middle panel), but no (new) periodic points of least period $k = 8$. Thus, in this case, Theorem 3.8 implies that the dynamics exhibit periodic behavior of periods $k = 4, 2$ or $k = 1$ (convergence).

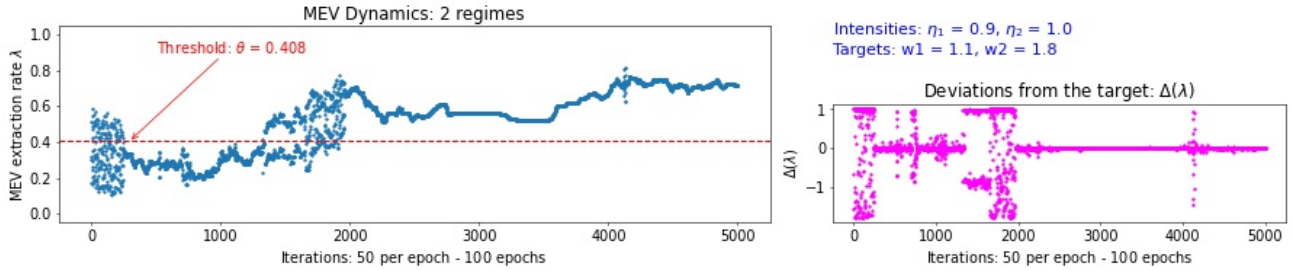

Figure 4: In this scenario, we consider a two-regime market with a threshold $\theta = 0.408$ on the extraction rate governing the transition. We handle two control parameters based on the current extraction rate. The left panel shows the evolution of (MEV-D) **for 5,000 iterations, which is divided in groups of 100 epochs. The right panel shows the deviations from the target $\Delta(\lambda)$ during those 100 epochs.**

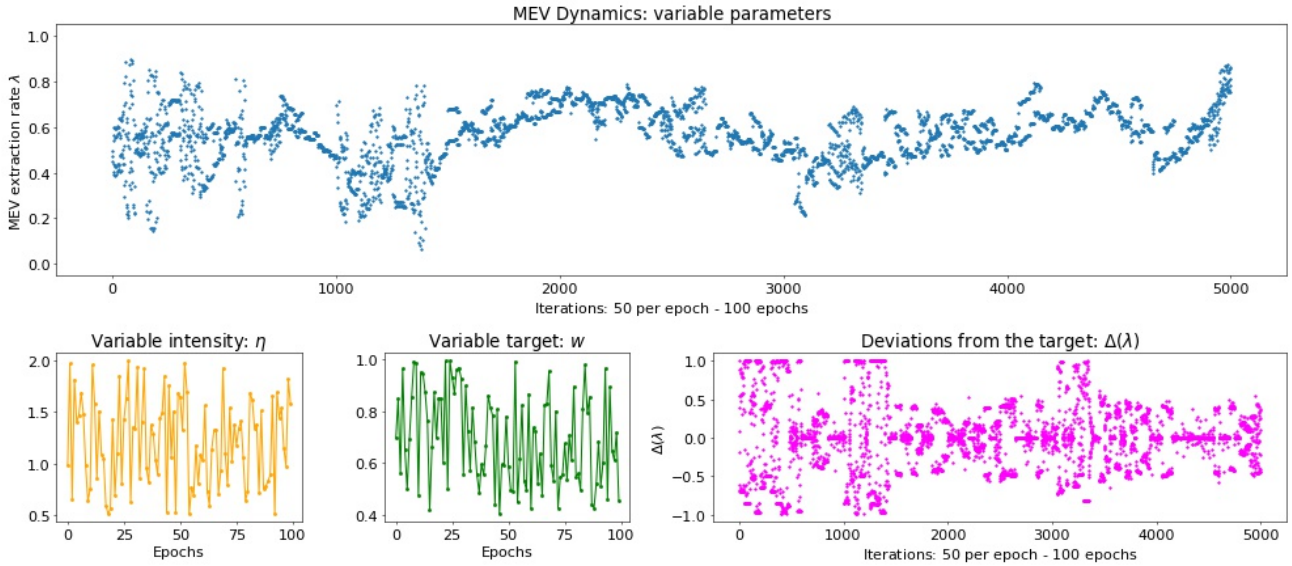

Figure 5: In this scenario, we consider an adversarial setting where the intensity of the updates and the target is randomly sampled in each epoch. The upper panel shows the evolution of (MEV-D) **in 5000 iterations, that is divided in 100 epochs. The bottom left panel shows the control parameters randomly drawn over the 100 epochs. The middle panel shows the target values drawn over the 100 epochs. The right panel shows the deviations $\Delta(\lambda)$ from the target over the 5000 iterations**